J. Geophys. Res. Vol. 115, A09314 doi:10.1029/2010JA015531

Ionospheric Holes made by Ballistic Missiles from North Korea Detected with a Japanese Dense GPS Array

Masaru Ozeki and Kosuke Heki

Dept. Natural History Sci., Hokkaido University, N10 W8, Kita-ku, Sapporo 060-0810, Japan

(submitted 5 April, accepted 19 May, 2010, published 17 September)

Abstract

A dense array of Global Positioning System (GPS) receivers is a useful tool to study ionospheric disturbances. Here we report observations by a Japanese GPS array of ionospheric holes, i.e. localized electron depletion. They were made by neutral molecules in exhaust plumes (e.g. water) of ballistic missiles from North Korea, Taepodong-1 and -2, launched on August 31, 1998, and April 5, 2009, respectively. Negative anomaly of electron density emerged ~6 minutes after the launches in the middle of the Japan Sea, and extended eastward along the missile tracks. By comparing the numerical simulation of electron depletion and the observed change in ionospheric total electron content, we suggest that the exhaust plumes from the Taepodong-2 second stage effused up to ~1.5 x 10^{26} water molecules per second. The ionospheric hole signature was used to constrain the Taepodong-2 trajectory together with other information, e.g. coordinates of the launch pad, time and coordinates of the first stage splashdown, and height and time of the second stage passage over Japan. The Taepodong-2 is considered to have reached the ionospheric F region in ~6 minutes, flown above northeastern Japan ~7 minutes after the launch, and crashed to the Pacific Ocean without attaining the first astronautical velocity. Ionospheric hole in the 1998 Taepodong-1 launch was much less in size, but it is difficult to compare directly the thrusts of the two missiles due to uncertainty of the Taepodong-1 trajectory.

1. Introduction

It was in 1959 that *Booker* [1961] first detected a localized reduction of ionization by an exhaust plume of the Vanguard II rocket with ionospheric sounding. After the 1973 Skylab launch, *Mendillo et al.* [1975] found a sudden decrease in Total Electron Content (TEC) by measuring the Faraday rotation of radio signals from a geostationary satellite, and suggested that the exhaust plume of the

rocket chemically influenced the ionosphere. They inferred that water (H_2O) and hydrogen (H_2) molecules in the exhaust plume became positive ions by reacting with ambient oxygen ions, and their dissociative recombination with electrons caused the formation of an “ionospheric hole”. Later, active experiments of making such holes have been performed with dedicated burns of orbital maneuver systems (OMS) of Space Shuttle [e.g. *Bernhardt et al.,* 1988a,b; 2005] in order to study physical processes of the formation and decay of the holes.

Past observations are based on limited numbers of ground stations with special equipments including cameras to record airglows and incoherent scatter radars to profile electron densities [*Mendillo et al.*, 1987; *Bernhardt et al.*, 1998]. Over the last two decades, many continuous Global Positioning System (GPS) receiving stations have been deployed worldwide to measure crustal movements. They enabled cheap and easy measurements of TEC using the phase difference of the two L band carrier waves from GPS satellites. Such GPS-TEC measurements have been contributing to study disturbances in ionosphere, e.g. sudden increase of TEC by solar flares [*Zhang and Xiao*, 2005], decrease by solar eclipse [*Afraimovich et al.*, 2002], the aftermath of geomagnetic storms [*Mitchell et al.,* 2005], medium-scale traveling disturbances excited by solar terminator [*Afraimovich et al.*, 2009], and so on.

In regions of high crustal activity, such as Japan and western USA, dense GPS arrays have been established. High spatial resolution observations with such arrays revealed properties of propagation of various kinds of traveling disturbances in ionosphere [*Saito et al.*, 2002; *Heki and Ping*, 2005; *Tsugawa et al*., 2007; *Astafyeva et al.*, 2009]. In 2006, a Japanese dense GPS array GEONET (GPS Earth Observation Network) [see e.g. *Heki*, 2004] detected the growth and decay of an ionospheric hole associated with the launch of an H-IIA rocket [*Furuya and Heki*, 2008]. However, it flew southward from an island in southern Japan, and they could not fully exploit the high density of GPS stations.

So-called Taepodong-1, and -2, multiple stage ballistic missiles (or launch vehicles according to the North Korean government) with possible liquid fuel engines, were launched from Musudanri, on the eastern coast of North Korea, on August 31, 1998, and April 5, 2009, respectively. In both cases, their first stages splashed down onto the Japan Sea, and the second stages flew over northeastern (NE) Japan and crushed in the Pacific Ocean [see, e.g. *Brumfiel*, 2009]. Although the North Korean government announced that these rockets successfully put communication satellites into orbit, they have not been confirmed [*US Northern Command*, 2009].

Whatever they actually are, their details, e.g. specifications, trajectories, have not been publicized by the North Korean authorities. The Japanese and American governments are considered to have captured them with their military radar and satellite systems, but only limited parts of their details

have been disclosed to public. Here we try to study their ionospheric hole signatures using a Japanese dense GPS network, a purely civilian sensor with data open to public (www.gsi.go.jp/ENGLISH). Here, as a challenge in application of space physics, we will try to extract as much useful information as possible, e.g. their trajectories and thrusts, from the Japanese GPS data.

2. Launches and trajectories of Taepodong-1 and -2

Taepodong (called as Pekdosan in North Korea) is a series of two or three-stage ballistic missiles (or rockets) launched from North Korea. Those launched in August 1998 and April 2009 from Musudanri are often called the Taepodong-1 and -2 (referred to as T-1 and T-2 hereinafter). Their specifications are not made available to public, and have been inferred from various pieces of information such as photographs from satellite, tracking by military radars, and TV news broadcasted in North Korea. T-1, in its 1999 launch, might have carried a third stage that was supposed to put a small satellite into a low Earth orbit. Radar tracking data by the US government suggest that the first two stages worked but the third stage has exploded without injecting a satellite into orbit. Western analysts believe that T-1 is ~26 meter long with an initial weight of ~21 tons and able to deliver a one ton payload to a range of ~2500 kilometers [e.g. *Hildreth*, 2008]. No information on the 1999 T1 trajectory has been known except that it was launched at 03:07UT, August 1998.

The first test of T-2, ~36 meters long, ended as a failure in July 5 2006 without reaching ionospheric height. Finally, T-2 was launched at 02:30UT, 5 April, 2009. Its first stage fell onto the middle of the Japan Sea (43°35’N 135°58’E), where an aircraft of the Japanese Marine Self Defense Force found a trace on the sea surface shortly after the launch. The second stage (and possibly the third stage and the payload) fell into the Pacific Ocean. No object entered orbit, either [*Brumfiel*, 2009].

The 2009 T-2 is relatively rich in information on its trajectory. It mostly came from the public release of the information obtained with radar tracking by the Japanese Ministry of Defense (MOD). These “constraints” are summarized in Table 1. In Fig.1, we plot height and horizontal travel distance against the time after launch for a trajectory adjusted to satisfy these constraints. Errors given in Table 1 are more or less arbitrary, and inferred from various sources. For example, the passing height of the second stage over Japan was reported as 370-400 km in the official statement made on 25 May 2009 [*MOD*, 2009], so we treated this constraint as 385 ± 15 km. Time of splashdown of the first stage is reported just as “around 02:37UT”, and so we assumed it 7.0 ± 0.5

minutes after the launch. *MOD* [2009] also announced that the second stage passed over Japan "around 02:37UT" (7.0 ± 0.5 minutes after the launch). We considered the approximate horizontal velocity (~4 km/sec), and gave the error of ±120 km (distance it travels in 0.5 minutes) to the horizontal travel distance of 970 km (approximate distance of NE Japan from the launch pad) at 7 minutes after the launch.

For both stages, acceleration was assumed to linearly increase reflecting the decreasing mass of remaining fuel. We also assumed that the missile attitude was controlled so that the elevation angle of the trajectory decreased smoothly from 90 degrees at the launch time with constant rates. As summarized in Table 2, eight parameters were tuned by grid search so that they minimize the square sum of the differences between the "simulated" and the "observed" values, normalized by their uncertainties, of the six items in Table 1. The time of the first engine jettison, inferred in this way, is 2.6 minutes after the launch, when T-2 was below 100 km. Consequently, it should be the second stage that penetrated the ionosphere. The first stage after the jettison and the second stage after the engine stop are assumed to have fallen freely without air drags. We did not constrain the splashdown point of the second stage in the Pacific Ocean because its precise coordinate is not available. Time of the stop of the second stage engine (6.5 minutes after the launch) is partly constrained by the eastern extent of the ionospheric hole as discussed in Section 4.3.

The estimation of the T-2 trajectory is such a rough one based on numbers of simplified assumptions. The obtained trajectory may not be a unique one, but its basic scenario, e.g. separation of the first stage below the ionosphere, the second engine stop before passing over Japan, would remain the same. The inferred trajectory satisfies the constraints pretty well as seen in Table 1 and Fig. 1. We gave a subtle curve for the trajectory (convex to the north) so that it smoothly traces the ionospheric hole as shown in Section 3. The purpose of this estimation is to enable simulation of the ionospheric hole for T-2 using a realistic trajectory as explained in Section 4. Hence, rigorous statistical discussion on the accuracy of the estimated trajectory is beyond the scope of this study. For the T-1 launch 1999, we do not have good constraints on its trajectory. So we will limit discussion within the comparative studies of ionospheric hole signatures between T-1 and -2.

3. GPS Data analysis

3.1. Isolation of anomalous TEC changes

The Japanese dense GPS array GEONET is composed of ~1000 continuous GPS tracking stations, and records L-band carrier phases in two frequencies, 1.5 (L1) and 1.2 GHz (L2), every 30 seconds. We downloaded the raw data on the day of the T-1 and -2 launches available on line from the Geographical Survey Institute, Japan. Temporal changes of the differences between the two phases

expressed in lengths are proportional to changes in TEC. At first, we will have a look at a pair of satellite 29 and GPS station 0232 (Ryotsu, Niigata), whose line-of-sight (LOS) penetrates the ionosphere due east of the launch pad. Fig.2 (dark gray curve) shows the time series of TEC over a two hours period including the 2009 T-2 launch. There TEC shows an abrupt dip 5-6 minutes after the launch, and gradual recovery in half an hour or so. To isolate the anomalous change of TEC, we model the raw TEC as a function of time t and angle ζ between LOS and the local zenith at its ionospheric penetration point (IPP) with a model,

$$\mathrm{TEC}(t,\ \zeta) = \mathrm{VTEC}(t)/\cos\zeta + d, \quad (1)$$

where VTEC (Vertical TEC) is the TEC when LOS is perpendicular to the ionosphere. The bias d inherent to phase observables of GPS remains constant for individual satellites in the studied period. VTEC can be separated from d with a few hours of observations because ζ varies with time as the satellite moves in the sky (ζ can be calculated easily from orbital elements of GPS satellites). VTEC changes diurnally, and its change in the two hours period can be well approximated with a quadratic function of t, that is,

$$\mathrm{VTEC}(t)=at^2 + bt + c. \quad (2)$$

We estimated a,b,c and d using the least-squares method (40 minutes period 02:30-03:10UT, influenced by the ionospheric hole, was excluded when we estimated these parameters), and the estimated model is shown in Fig.2 with a smooth curve in medium gray. The TEC anomaly was derived as the difference between the model and the observed raw TEC. Fig.2 shows that the anomaly is characterized by a sudden dip of ~3 TEC Unit (TECU, 1TECU = 10^{16} electrons/m^2) starting at 02:35:30UT (5.5 minutes after the launch). This anomalous decrease lasts for nearly half an hour.

3.2. Ionospheric hole

Fig.3 shows the map projection of the emergence of the ionospheric hole by T-2. We show VTEC anomalies, derived by multiplying TEC anomalies by cosζ, because they are suitable to compare the hole signatures derived by different satellites. They show three different epochs, i.e. 2:35:00UT, 2:35:30UT, and 2:36:00UT, which correspond to 5.0, 5.5, and 6.0 minutes after the launch, respectively. The dots show sub-ionospheric points (SIP), ground projection of IPP. Their colors are dominated by green (normal), with some yellow/red and blue dots indicating positive and negative anomalies, respectively. The SIP positions are calculated assuming a certain height of a thin

ionosphere, and the height is normally taken at the maximum ionization height (~300 km in the case of 2009 T-2 launch, see ionospheric sounding data at World Data Center for Ionosphere, http://wdc.nict.go.jp/). In the present case, however, the disturbance is localized at a particular height. Therefore we used a slightly lower altitude 265 km, the height of the T-2 trajectory (i.e. height of the ionospheric hole) at ~6 minutes after the launch (see the discussion in the next paragraph) in order to show the proper ground projection of the hole.

No large anomalies are seen 5 minutes after the launch (Fig.3a). There are weak positive anomalies around the Russian coast. Although we do not know their origin, they are probably irrelevant to T-2. A distinct negative TEC anomaly emerges ~5.5 minutes after the launch (Fig.3b), and grew eastward reaching the middle of the Japan Sea ~30 seconds later (Fig.3c). These are considered to be the initial stage of the ionospheric hole formation by the exhaust plume of T-2.

Next we try to constrain the height of the ionospheric hole around the center of the Japan Sea (41N 136E, ~530 km from the launch pad). The latitude and longitude of SIP depend on the assumed height of the thin ionosphere, i.e. lower or higher altitudes result in SIP closer to or farther from the GPS station, respectively (Fig.4). Now we assume that an ionospheric hole is observed with multiple GPS satellites from GPS stations at various parts of the array. If their SIPs are derived with correct heights, the hole signatures from different satellites should overlap (Fig.4b). Fig.5 shows SIPs calculated with ionospheric altitudes of 240 km (a), 265 km (b), and 290 km (c). The negative anomalies by satellites 29 and 15 are more continuous in space in (b) than in (a) and (c). Hence the ionospheric hole in the middle of the Japan Sea would have been as high as ~265 km, that is, the second stage of T-2 should have reached this altitude when it traveled ~530 km from the launch pad in 6 minutes after the launch (time lag between the missile passage and the hole formation is considered small, see Section 4.3). This constitutes the second and the third constraints in Table 1.

4. Model of the ionospheric hole formation by Taepodong-2

4.1 Pre-launch conditions

In the dayside ionosphere, electrons are continuously produced by several processes, including the photoionization of atomic oxygen by solar radiations in ultraviolet and x-ray. The production rate f depends on the altitude z and the solar zenith angle θ. On the other hand, recombination of O^+ and e^-, involving intermediate reactions with neutral molecules, lets electrons decay naturally at a rate proportional to the electron density $n(e^-)$, i.e.

$$\frac{dn(e^-)}{dt} = -\beta_{eff} \cdot n(e^-) + f(z,\theta). \quad (3)$$

The coefficient β_{eff} is about 1.98 x 10^{-5} at the F layer height [*Mendillo et al.*, 1975]. The dependence of f on θ results in diurnal variations of TEC. Its height dependence results in the Chapman distribution (Fig.1a) [*Chapman*, 1931] expressed as

$$n(e^-) \propto \exp\frac{1-\xi-\exp(-\xi)}{2} \qquad \xi \equiv \frac{z-h_c}{H} . \tag{4}$$

There h_c is the height of maximum ionization, and was ~300 km in the studied area and time (see the previous section). The scale height H was taken as 65 km [*Calais et al.*, 1998]. Daily values of VTEC, the vertical integration of $n(e^-)$, are routinely obtained from GEONET data and made available on line from Kyoto University (Akinori Saito, www-step.kugi.kyoto-u.ac.jp/~saitoua/GPS_TEC). They show that the background VTEC was ~12 TECU around the time and place of the T-2 launch, and we scaled the $n(e^-)$ profile so that VTEC takes that value. Here we assume quasi-equilibrium, i.e., $f \approx \beta_{eff} \cdot n(e^-)$. So the electron density would have been nearly stationary during the studied period (~30 minutes) if the T-2 launch had not taken place.

The exhaust plume of a rocket or a missile brings large amounts of neutral molecules into the ionosphere. In the case of H-IIA rockets, the main constituent of the exhaust is H_2O [*Furuya and Heki*, 2008]. The second stages of the Taepodong series, which largely inherit the Scud missile technology of the former Soviet Union, are inferred to use liquid fuel, e.g. unsymmetrical dimethyl-hydrazine (UDMA, $N_2C_2H_8$), and nitric acid as the oxidizer. Their chemical compositions suggest that about a quarter of the exhaust plume in weight is H_2O. Water molecules encourage chemical recombination between O^+ and e^-, and make an ionospheric hole. Following *Furuya and Heki* [2008], we simulate this process in two steps, i.e. diffusion of H_2O from the plume, and dissociative recombination of molecular ions and e^- (the two steps actually occur simultaneously). Then we calculate TEC signals expected in actual GPS satellite-receiver pairs whose LOSs penetrate the hole. In the exhaust, there should be minor amount of CO_2 and H_2, which would also contribute to the hole formation. We consider only water in the simulation, and discuss this issue in the Section 4.3.

4.2 Diffusion of H_2O

Water molecules in the exhaust plume rapidly diffuse into the atmosphere. The initial velocity of the T-2 exhaust relative to the ambient atmosphere, which can be calculated from the specific

impulse, is unknown. Fig.1 shows that the velocity is ~4 km/sec when T-2 started to make an ionospheric hole (5-7 minutes after the launch). This is close to the exhaust effusion velocity of the H-IIA first stage [*Furuya and Heki*, 2008]. Here we assume that the T-2 second stage has a similar gas effusion velocity. Then T-2 is almost as fast as the exhaust effusion, and we can neglect initial velocity of water molecules. Even if they have initial velocity of up to a few km/sec, it would not much influence the simulation because the typical travel distance of non-collisional flow, which precedes the onset of diffusion, would not exceed a few tens of kilometers under the present situation [*Bernhardt*, 1979b].

The molecule density at a certain radial distance diffused from a point source can be calculated easily by using the spherical diffusion formula as given in e.g. *Mendillo et al.* [1975]. However, the diffusion constant actually increases with altitude. For example, diffusion constants of water molecules at altitudes 250, 350, and 450 km are about 2, 12 and 67 km^2/second, respectively [*Mendillo et al.*, 1975]. In order to take account of faster/slower diffusion upward/downward, we calculated the density of water molecule $n(H_2O)$ using the approximate expression of such anisotropic diffusion from a point source given in *Bernhardt* [1979a].

Furuya and Heki [2008] inferred the number of H_2O molecules released in unit time from the specifications of the H-IIA first stage; the mass of the gas put into atmosphere in a second is obtained by dividing the thrust (1.073×10^6N) with the specific impulse (429 seconds). Given the weight of an H_2O molecule, they obtained the number as 8.5×10^{27} per second. Considering that (1) the length of the T-2 second stage is about a half of the H-IIA first stage, (2) exhaust gas made by the reaction between UDMA and nitric acid would include ~1/4 of water vapor in weight, we inferred that the T-2 second stage would have effused water molecules ~2 percent of the H-IIA first stage in a unit time (i.e. $\sim 1.7 \times 10^{26}$ per second).

Here we assumed that other neutral molecules in the exhaust gas (e.g. H_2 and CO_2) do not contribute to electron depletion. Following *Furuya and Heki* [2008], we approximated continuous gas effusion from the missile with a series of discrete point sources put along the track with a 10 second separation. The water density $n(H_2O)$ at a certain point was calculated as the sum of $n(H_2O)$ from these set of point sources. Because the first stage engine was separated below 100 km, we only considered the second stage engine from altitude of 100 km until it stops at 6.5 minutes after the launch.

4.3 Formation of the hole and penetration of line-of-sights

Artificially added water molecules react with O^+ and become H_2O^+, whose dissociative recombination with e^- causes electron depletion. By adding this loss term to equation (3), $n(e^-)$ after

the launch would change as

$$\frac{dn(e^-)}{dt} = -\beta_{eff} \cdot n(e^-) + f(z,\theta) - \beta_{H_2O} \cdot n(e^-) \quad . \tag{5}$$

Here we assume that β_{H2O} is proportional to the water density, i.e. β_{H2O} = 2.2 x 10^{-15} x $n(H_2O)$ [*Mendillo et al.*, 1975].

We followed *Furuya and Heki* [2008] to model the electron density changes. We set up a three dimensional grid over the rectangular area 1500 km x 1500 km covering the T-2 trajectory, and 150-700 km in altitude, with 30 km horizontal and 10 km vertical separations. We let the electron densities at the grid points evolve in time following equation (5) with a time step of 15 seconds in response to the changing $n(H_2O)$ and $n(e^-)$. The electron density profiles at selected epochs show almost instantaneous emergence and rapid expansion of the hole from the trajectory (Fig.7).

Next we simulate TEC variations in the actual geometry of GPS satellites and stations. At first we calculate slant TEC time series at selected GPS stations. We repeated the following steps every 30 seconds for each of the five GPS stations 0232, 0564, 0198, 0200, and 0203 (Fig.8). We first calculated the position of satellite 29 in the Earth fixed frame using broadcast orbit, and secondly calculated $n(e^-)$ along the LOS at altitudes 150-700 km in 10 km steps by interpolating from values at grid points, and finally the values are integrated to obtain slant TEC at the epoch. In Fig. 8, we plot anomalies (difference from normal values) in slant TEC. There we can see that the first ten minutes, simulated changes agree well with the observations. Here we tuned the number of water molecules in the exhaust plume to ~1.5 x 10^{26} per second (~1.8 percent of those from the H-IIA first stage) (Fig.9). This is close to our initial guess of 1.7 x 10^{26}.

This number needs be modified downward if we consider other kinds of chemically reactive molecules, e.g. H_2, CO_2, in the exhaust plume. For example, the Skylab exhaust included ~30 percent of H_2 molecule in addition to water [*Mendillo et al.*, 1975], and the Shuttle OMS burn releases H_2, CO_2 molecules in addition to water [*Bernhardt et al.*, 1988a,b]. Chemical composition of UDMA suggests that the Taepodong series exhaust may include some amount of H_2 and CO_2, in addition to H_2O. Quantitative assessment is difficult without chemical analyses of the actual exhaust gas, but their existence would cause overestimation of water molecules (because a part of the hole was made by these non-water molecules). H_2 and CO_2 have different diffusion constants and different speeds of chemical reaction with oxygen ions [*Bernhardt*, 1987]. Hence their presence will slightly modify the shapes of the synthesized curves of TEC changes in Fig.8 as well.

As the next step, we calculate vertical TEC anomalies for all the GPS stations at three selected epochs. Fig. 6 compares geographical distribution of the observed VTEC anomalies (a-c) with the simulated anomalies (d-f). They agree fairly well. Fig. 8 suggests that the agreement worsen after the

first ten minutes, i.e. observations show a somewhat shorter life of the hole than the simulations. As discussed in *Furuya and Heki* [2008], the equation (5) neglects several factors for the ionospheric hole decay. One such factor would be the inward electron flow, and this might have been responsible for these discrepancies. *Bernhardt et al.* [2001] reported that the hole made by the OMS burn above Peru recovered within 10 minutes, much faster than the present case. This might reflect the fact that holes in equatorial regions may decay faster because electrons can flow horizontally into the hole there owing to small inclination of the geomagnetic field.

As seen in Figs.6c and 6f, the ionospheric hole does not cover Honshu although T-2 flew over that island. Actually, the eastern end of the hole barely overlaps with the land area. As seen in Table 2, the second stage is assumed to have stopped at 6.5 minutes after the launch, i.e. shortly before it passes over Japan. This is an important fact deduced from the ionospheric hole signatures. Because the second stage (and maybe the third stage and the payload) correctly fell within the area prescribed by the North Korean government as the dangerous region ~2100 km east of Honshu [*MOD*, 2009], this engine stop would not have been accidental. Anyway, the velocity of the second stage at the time of the engine stop is far less than the 7.9 km/sec, the first astronautical velocity. Hence further acceleration by the third stage, if any, would have been indispensable to put a payload into the orbit. With the current data, it is difficult to tell whether the experiment failed (i.e. failure in the separation and ignition of the third stage) or succeeded (i.e. successful demonstration of the capability of the missile to deliver a warhead to a range of thousands of kilometers).

5. Comparison with the Taepodong-1

There is nearly no information on the trajectory of T-1, launched on 1998 August 31, except the approximate launch time of 03:07UT. We performed similar analyses to T-2, and found that it also made an ionospheric hole ~6 minutes after the launch. Fig.10 shows the hole made by T-1 observed with satellite 6 (other satellites were not available with suitable LOS). The area covered by the negative anomalies is much smaller than T-2, suggesting less water molecules included in the exhaust plume of T-1. The time series at five GPS stations (Fig.11) showed TEC decrease of 2-3 TECU, one half or so of the T-2. They also show faster recovery of TEC than those in the T-2 case (Fig.8), although this is due partly to the smallness of the ionospheric hole, i.e. movement of GPS satellites in the sky let LOS move away from the hole quicker than in the T-2 case.

The T-1 launch is ~11 years before T-2, i.e. they are almost at the same phase of the solar cycle. The local time of the T-1 launch is only 37 minutes later than T-2. Consequently, we expect that the background TEC were similar in the 1998 and the 2009 cases. However, daily VTEC changes by A. Saito (see Section 3.1 for URL) show that the background VTEC was ~24 TECU at the time of the

T-1 launch, nearly twice as large as in the T-2 launch. So TEC would have decreased more in 1998 Aug. 31 than in 2009 April 5 if the same amount of water molecules were released. This is demonstrated in Fig.9, where approximately twice as large TEC decrease occurs under twice as large background TEC.

Fig. 11 shows that the largest TEC decrease is ~3 TECU. Unfortunately, the T-1 trajectory is not well known, and it is impossible to directly compare this with Fig.8. Here we assume that their trajectories (including the jettison of the first stage) were similar, and that LOS connecting the satellite 6 and the GPS station showing the largest TEC decrease (0196) intersects the hole in a similar geometry to the T-2 case of the satellite 29 and the station 0203 (Fig.8). Then, Fig.9 suggests that the number of water molecule from T-1 is ~2.6×10^{25} per second i.e., ~0.3 percent of the H-IIA first stage. This corresponds to ~1/6 of the 2009 T-2 case. T-1 is inferred to be ~26 m tall, about 5/7 of T-2 (~36 m) (information available, e.g. at http://en.wikipedia.org/wiki/Taepodong-2). A length contrast of 5:7, however, may not be strong enough to explain the 1:6 contrast in thrust (assuming their similarity in shape). This might suggest either that the missile technology in North Korea has progressed (i.e. more thrust per unit volume of missile), or that the chemical components of the fuel are different between the T-1 and -2 second stages.

6. Conclusions

Here we studied ionospheric signatures of the two ballistic missiles from North Korea with a dense GPS array in Japan. We had to rely on lots of uncertain information on the missile themselves and their trajectories because of the classified nature of the affairs. However, with civilian data from the GPS array, we could conclude as follows.

1) Ionospheric holes made by the launches of T-1 in 1998 and T-2 in 2009 from North Korea were identified by a Japanese dense GPS network. They emerged ~6 minutes after the launches as the E-W elongated regions of negative TEC anomalies in the middle of the Japan Sea.
2) For T-2, we found a trajectory mostly consistent with available constraints, and this trajectory enabled us to reproduce the formation of the ionospheric hole by numerical simulation. Information from the ionospheric hole also helped us constrain the trajectory.
3) The second stage of T-2 is considered to have effused ~1.5×10^{26} water molecules (or less if there are considerable amount of H_2 and CO_2 in the exhaust) per second. The eastern limit of the hole suggests that the engine stopped ~6.5 minutes after the launch before achieving the first astronautical velocity.
4) Amounts of the largest decreases of slant TEC were ~5 and ~3 TECU, in the T-2 and -1 launches, respectively. However, we have to take account of the differences in background TEC and

chemical compositions of fuel, and uncertainty of the T-1 trajectory, in order to compare their thrusts.

Acknowledgements

We thank the two reviewers for constructive comments, and Geospatial Information Authority of Japan (former Geographical Survey Institute) for making GEONET data available on line.

References

Afraimovich, E.L., E.A. Kosogorov, and O.S. Lesyuta, Effects of the August 11, 1999, total solar eclipse as deduced from total electron content measurements at the GPS network, *J. Atmos. Solar-Terrestrial Phys.*, *64*, 1933-1941, 2002.

Afraimovich, E.L., I.K. Edemskiy, A.S. Leonovich, L.A. Leonovich, S.V. Voeykov, and Y.V. Yasyukevich, MHD nature of night-time MSTIDs excited by the solar terminator, *Geophys. Res. Lett.*, *36*, L15106, doi:10.1029/2009GL039803, 2009.

Astafyeva, E., K. Heki, V. Kiryushkin, E. Afraimovich, and S. Shalimov, Two-mode long-distance propagation of coseismic ionosphere disturbances, *J. Geophys. Res.*, *114*, A10307, doi:10.1029/2008JA013853, 2009.

Bernhardt, P.A., Three-dimensional, time-dependent modeling of neutral gas diffusion in a nonuniform, chemically reactive atmosphere, *J. Geophys. Res.*, *84*, 793-802, 1979a.

Bernhardt, P.A., High-altitude gas releases: transition from collisionless flow to diffusive flow in a nonuniform atmosphere, *J. Geophys. Res.*, *84*, 4341-4354, 1979b.

Bernhardt, P.A., A critical comparison of ionospheric depletion chemicals, *J. Geophys. Res,*, *92*, 4617-4628, 1987.

Bernhardt, P.A., B.A. Kashiwa, C.A. Tepley, and S.T. Noble, Spacelab 2 upper atmospheric modification experiment over Arecibo, 1, neutral gas dynamics, *Astrophys. Lett. Commun.*, *7*, 169-182, 1988a.

Bernhardt, P.A., W.E. Swartz, M.C. Kelley, M.P. Sulzer, S.T. Noble, Spacelab 2 upper atmospheric modification experiment over Arecibo, 2, plasma dynamics, *Astrophys. Lett. Commun.*, *7*, 183-198, 1988b.

Bernhardt, P.A., J.D. Huba, W.E. Swartz, and M.C. Kelley, Incoherent scatter from space shuttle and rocket engine plumes in the ionosphere, *J. Geophys. Res.*, *103*, 2239-2251, 1998.

Bernhardt, P. A., J.D. Huba, E. Kudeki, R.F. Woodman, L. Condori, and F. Villanueva, Lifetime of a depression in the plasma density over Jicamarca produced by space shuttle exhaust in the ionosphere, *Radio Sci.*, *36*, 1209-1220, 2001.

Bernhardt, P.A., P.J. Erickson, F.D. Lind, J.C. Foster, and B.W. Reinisch, Artificial disturbances of the ionosphere over the Millstone Hill Incoherent Scatter Radar from dedicated burns of the space shuttle orbital maneuver subsystem engines, *J. Geophys. Res., 110*, doi:10.1029/2004JA010795, 2005.

Booker, H.G., A local reduction of F-region ionization due to missile transit, *J. Geophys. Res., 66*, 1073-1079, 1961.

Brumfiel, G., Korean satellite misses orbit, *Nature, 458*, 685, 2009.

Calais, E., J.B. Minster, M.A. Hofton, and H. Hedlin, Ionospheric signature of surface mine blasts from Global Positioning System measurements, *Geophys. J. Int., 132*, 191-202, 1998.

Chapman, S., The absorption and dissociative or ionizing effect of monochromatic radiation in an atmosphere on a rotating earth, *Proc. Phys. Soc. (London), 43*, 26-45, 1931.

Furuya, T., and K. Heki, Ionospheric hole behind an ascending rocket observed with a dense GPS array, *Earth Planets Space, 60*, 235-239, 2008.

Heki, K., Dense GPS array as a new sensor of seasonal changes of surface loads, in *The State of the Planet: Frontiers and Challenges in Geophysics*, edited by R.S. Sparks and C.J. Hawkesworth, *Geophys. Monograph, 150*, 177-196, American Geophysical Union, Washington, 2004.

Heki, K. and J.-S. Ping, Directivity and apparent velocity of the coseismic ionospheric disturbances observed with a dense GPS array, *Earth Planet. Sci. Lett., 236*, 845-855, 2005.

Hildreth, S.A., North Korean ballistic missile threat to the United States, *CRS Rep. for Congress* RS21473, 2008.

Mendillo, M., G. S. Hawkins, and J. A. Klobuchar, A sudden vanishing of the ionospheric F region due to the launch of Skylab, *J. Geophys. Res., 80*, 2217-2225, 1975.

Mendillo, M., J. Baumgardner, D.P. Allen, J. Foster, J. Holt, G.R. A. Ellis, A. Klekociuk, and G. Reber, Spacelab-2 plasma depletion experiments for ionospheric and radio astronomical studies, *Science, 238*, 1260-1264, 1987.

Ministry of Defense, On the launch of a missile from North Korea, Official Statement on 15 May, 2009, http://www.mod.go.jp/j/library/bmd/20090515.html. (in Japanese)

Mitchell, C.N., L. Alfonsi, G. De Franceschi, M. Lester, V. Romano, and A. W. Wernik, GPS TEC and scintillation measurements from the polar ionosphere during the October 2003 storm, *Geophys. Res. Lett., 32*, doi:10.1029/2004GL021644, 2005.

Saito, A., M. Nishimura, M. Yamamoto, S. Fukao, T. Tsugawa, Y. Otsuka, S. Miyazaki, and M.C. Kelley, Observations of traveling ionospheric disturbances and 3-m scale irregularities in the nighttime F-region ionosphere with the MU radar and a GPS network, *Earth Planets Space, 54*, 31-44, 2002.

Tsugawa, T., Y. Otsuka, A. J. Coster, and A. Saito, Medium-scale traveling ionospheric disturbances detected with dense and wide TEC maps over North America, *Geophys. Res. Lett., 34*, L22101, doi:10.1029/2007GL031663, 2007.

United States Northern Command, NORAD and USNORTHCOM monitor North Korean launch, *U.S. Northern Command News*, April 5, 2009.

Zhang, D.H. and Z. Xiao, Study of ionospheric response to the 4B flare on 28 October 2003 using International GPS Service network data, *J. Geophys. Res., 110*, doi:10.1029/2004JA010738, 2005.

Table 1. Constraints on the Taepodong-2 missile trajectory.

Constraints (unit)	Simulated	Observed	Source of information
Horizontal distance at 6 minutes (km)	578.4	530.0 ± 50.0	This study
Height at 6 minutes (km)	294.2	265.0 ± 10.0	This study
Horizontal distance at 7 minutes (km)	855.3	970.0 ± 120.0	MOD radar[1]
Height at 7 minutes (km)	351.2	385.0 ±15.0	MOD radar[1]
Horizontal distance at splashdown (km)	517.1	530.0 ± 50.0	MOD visual observation[2]
Time of splashdown (minutes)	7.1	7.0 ± 0.5	MOD radar[1]
Total	Normalized Root-mean-square : 1.610		

[1]News release from Ministry of Defense on 15 May, 2009 [*MOD*, 2009].

[2]Splashdown point identified at (40°35'N 135°58'E) by the Japan Marine Self Defense Force P3C aircraft (red star in Fig.3c).

Table 2 Adjusted parameters of the trajectory of Taepodong-2.

Stage	Parameter	(unit)	Value (start)	Value (end)
First	burn time[1]	(min.)	0.0[3]	2.6[4]
	acceleration	(km/sec/min.)	0.18[4]	1.30[4]
	ascending angle[2]	(degree)	90.0[3]	33.3[4]
Second	burn time[1]	(min.)	(2.6)	6.5[4]
	acceleration	(km/sec/min.)	0.03[4]	1.50[4]
	ascending angle[2]	(degree)	(33.3)	11.9[4]
	# H_2O in exhaust	(per second)	1.5×10^{26}	

[1]Time after the launch, [2]This takes a value from 90.0 (vertically upward) to 0.0 (horizontal).

[3]Fixed to a-priori values. [4]Parameters adjusted by grid search to satisfy constraints in Table 1.

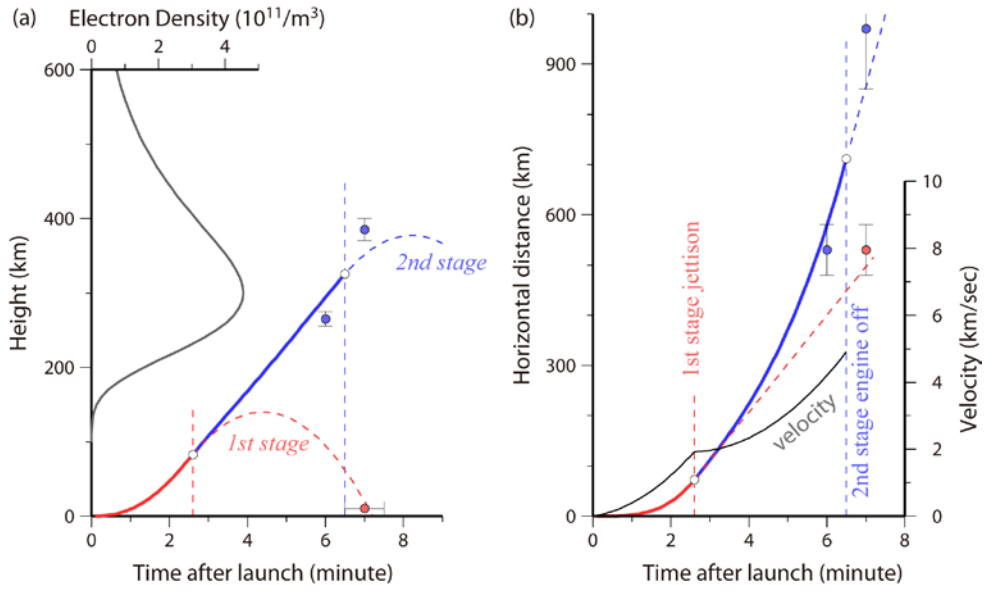

Figure 1. Height (a) and horizontal travel distance (b) of T-2 as functions of time after the launch. White dots at 2.6 after the launch denote separation of the first stage, and those at 6.5 shows the engine stop of the second stage. Dashed curves show the trajectories of the first (red) and the second (blue) stage engines after the jettison and the engine stop, respectively. Red and blue dots show the constraints for the first and the second stages, respectively, listed in Table 1. The gray curve in (a) shows the electron density as a function of height, modeled so that the peak density is at the height 300 km and vertical TEC becomes 12 TECU. The black curve in (b) shows the speed of the missile, which did not reach the first astronautical velocity of the Earth (~7.9 km/sec) by the stop time of the second stage engine.

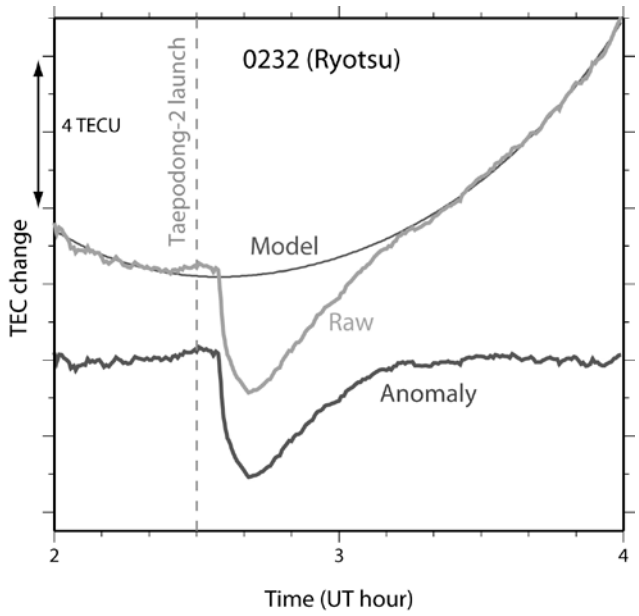

Figure 2. Raw time series (light gray) of slant TEC on 02-04UT, April 5, 2009, observed at 0232 (Ryotsu, Niigata, see Fig.8 for position) using the satellite 29. A smooth medium gray curve is the model composed of a constant bias and VTEC obeying a quadratic function of time (eqs. 1 and 2). Their difference was defined as the anomaly (dark gray). An unusual TEC decrease starts shortly after the launch of T-2 at 02:30UT.

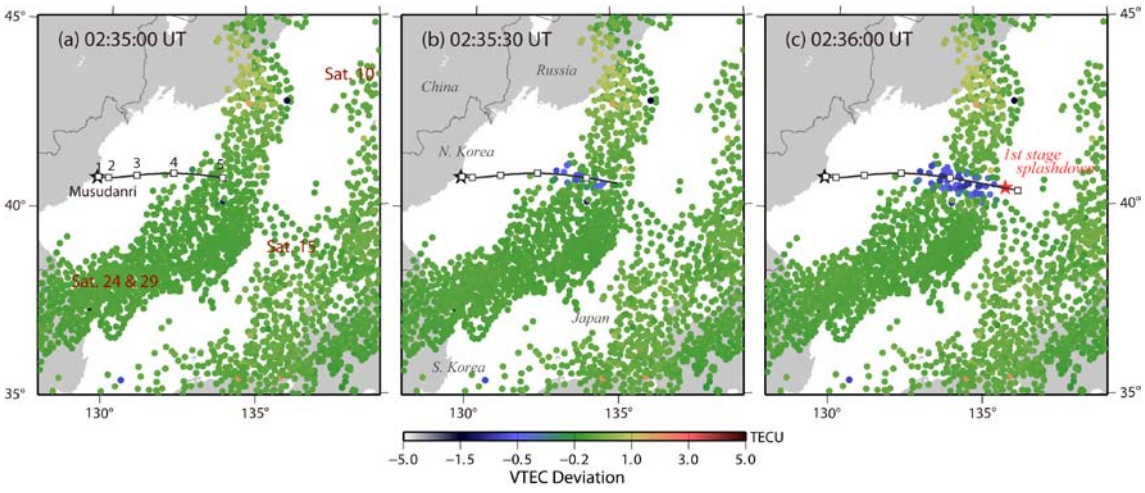

Figure 3. VTEC anomalies at (a) 2:35:00UT, (b) 2:35:30UT, and (c) 2:36:00UT, which correspond to 5.0, 5.5, and 6.0 minutes after the T-2 launch, respectively. Each dot corresponds to a GPS satellite and receiver pair (satellite numbers are shown in (a)). Electron depletion appear in (b) and grow eastward in (c) along the trajectory of the missile. Numbers attached to white squares along the trajectory (a) denote time in minutes after the launch. The red star in (c) shows the position of the splashdown of the first stage.

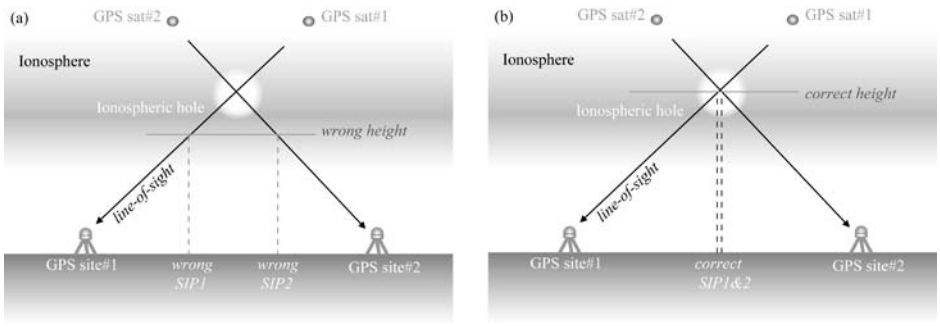

Figure 4. Because SIP positions depend on the assumed height of the ionosphere, it can be used to constrain the height of the observed anomaly. Two SIPs from two GPS satellites indicate different position of the hole if the assumed height is wrong (a). The true height can be constrained by bringing them to coincide (b).

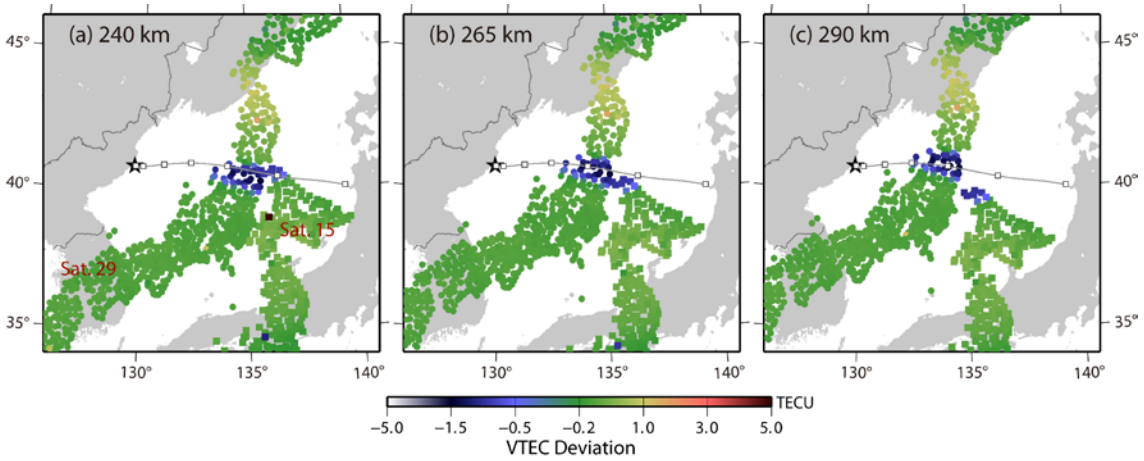

Figure 5. VTEC anomalies at 02:37, 7 minutes after the launch, obtained by two different GPS satellites 15 and 29, assuming the height of thin ionosphere of (a) 240 km, (b) 265 km, and (c) 290 km. The height 265 km (b) results in the smoother connection of the ionospheric hole signatures by the two satellites than 240 km (a) and 290 km (c).

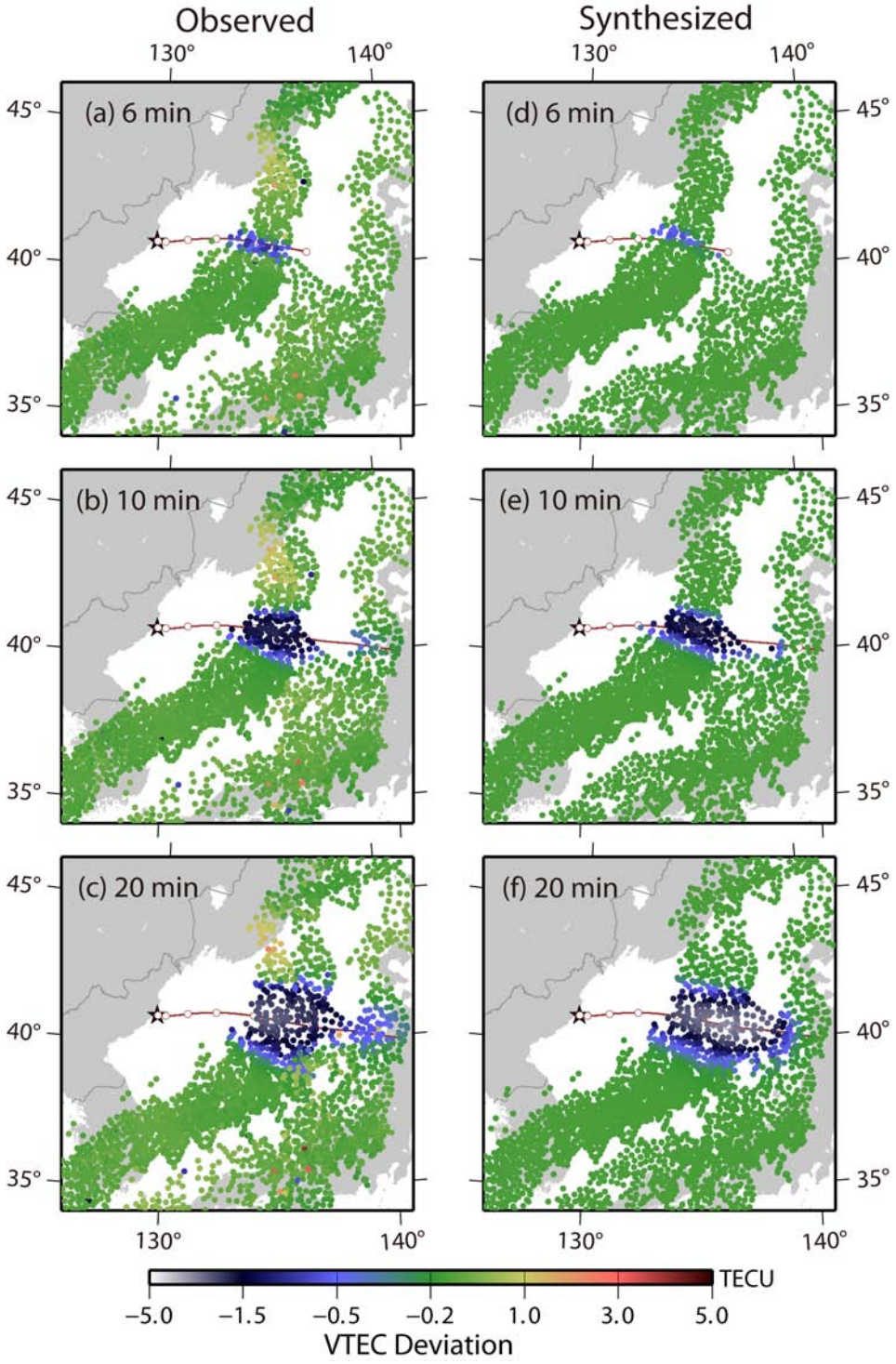

Figure 6. VTEC anomalies at 6 (a), 10 (b), and 20 (c) minutes after the launch of T-2, obtained by GPS satellites 10, 15, 24, and 29, are compared with those simulated in a computer (d-f). They have fairly similar distribution and amplitudes. The ionospheric hole does not extend to the Pacific coast of Honshu (c), suggesting that the second stage engine had stopped before its passage over Japan.

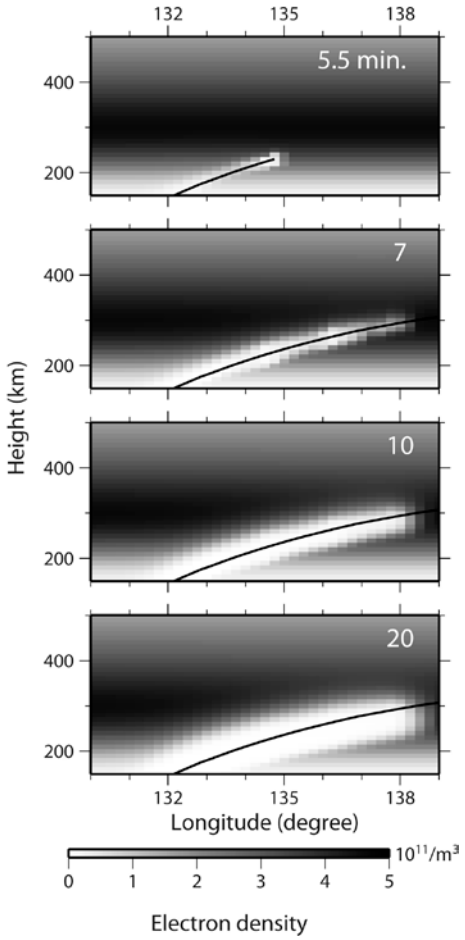

Figure 7. Snapshots at 5.5, 7, 10, 20 minutes after the launch of simulated growth of ionospheric hole along the T-2 trajectory (black curves). Vertical cross section along the latitude of ~40N with altitude range 150-500 km. Darkness indicates the density of electron, and ionospheric hole is recognized as the white part in the middle of the ionosphere. Background TEC was assumed to be 12 TECU with the density peak as high as 300 km (Fig.1a). Number of water molecules effused per second was set to 1.5×10^{26}, 1.8 % of the first stage of H-IIA. T-2 second stage engine was assumed to have stopped at 6.5 minutes after the launch (around 138E), so that the hole does not extend farther eastward.

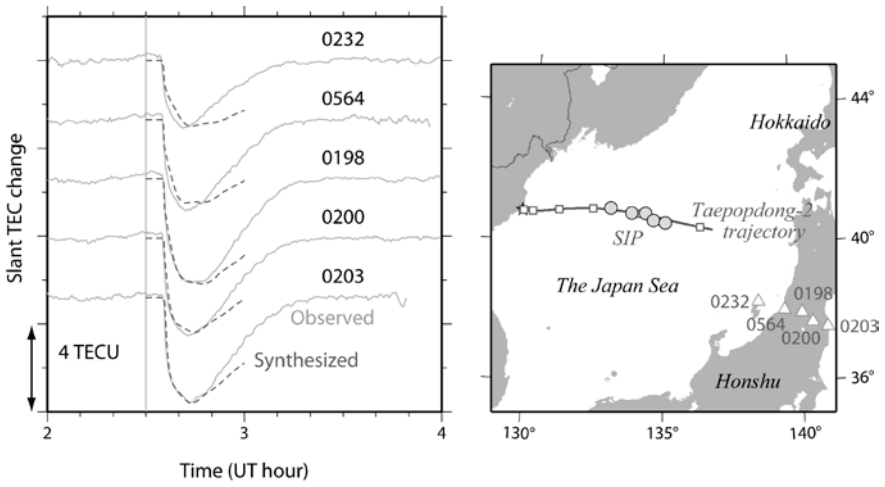

Figure 8. Time series of TEC anomalies at five GPS stations in Japan with GPS satellite 29 showing the appearance and decay of the ionospheric hole made by T-2. The map shows the SIP under the assumption of 265 km ionospheric height. These SIPs almost overlap with the trajectory. In the time series, we also show synthesized TEC changes (broken curves) assuming 1.5 x 10^{26} water molecules per second. The initial parts of the synthesized curves show TEC decreases consistent with the observations, but the decay of the hole (i.e. recovery of TEC) is not so well modeled (see text).

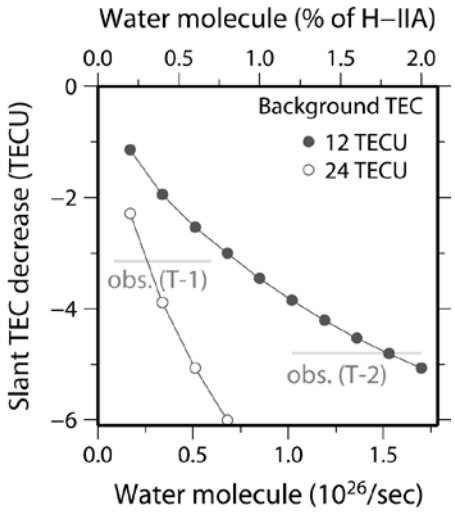

Figure 9. Relationship between the assumed number of water molecules effused in a second (upper horizontal axis shows those relative to the H-IIA first stage) and the TEC changes at the GPS station 0203 (Fig.8) for satellite 29. The background TEC was ~12 and ~24 TECU for the 2009 T-2 and the 1998 T-1 launches, respectively. The observed TEC decrease for this station-satellite pair after the T-2 launch (gray horizontal line) suggests that the number of water molecule in its exhaust gas is ~1.5 x 10^{26} per second. If we assume the T-1 situation similar to T-2 except the

background TEC, this value becomes ~0.26 x 10^{26} per second, or ~1/6 of T-2.

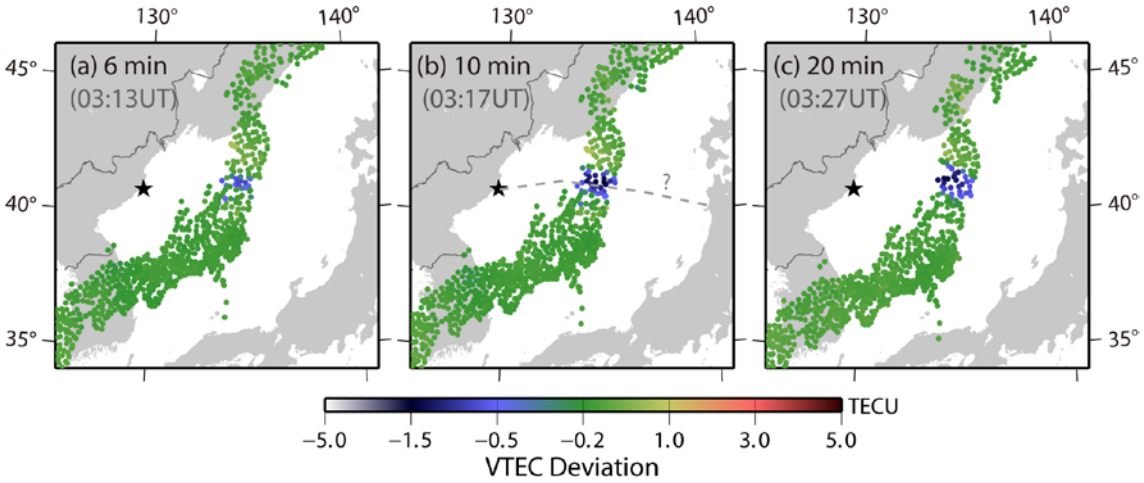

Figure 10. VTEC anomalies at (a) 03:13UT, (b) 03:17UT, and (c) 03:27UT, i.e. 6, 10, and 20 minutes after the T-1 launch, respectively. Each dot corresponds to a SIP of GPS receivers with the satellite 6. Electron depletion appears in the middle of the Japan Sea, but they are much smaller than the T-2 case (Fig.6a-c). A thin ionosphere was assumed at the height of 270 km to calculate SIP.

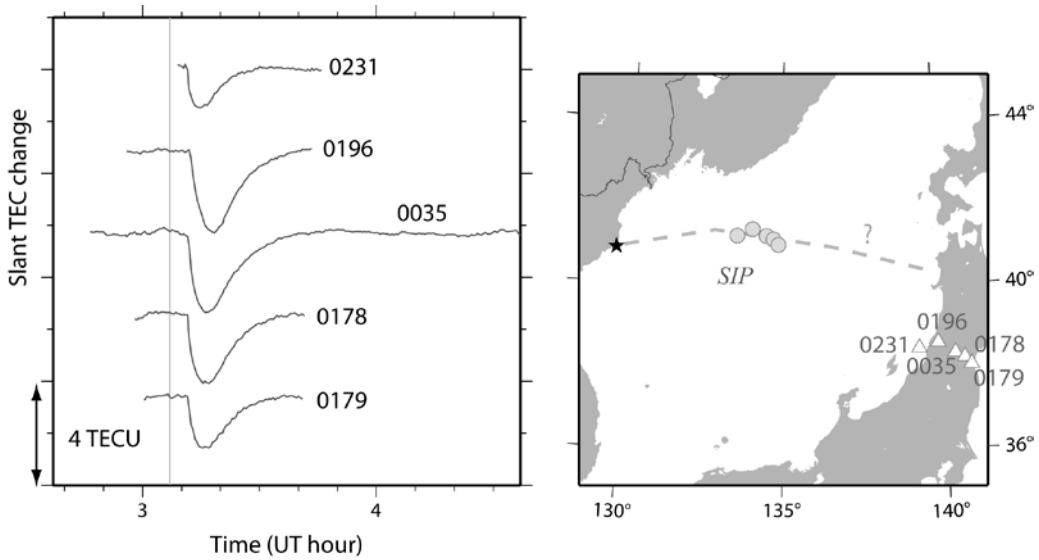

Figure 11. Time series of TEC anomalies at five GPS stations in Japan with the satellite 6 showing the emergence and decay of the ionospheric hole made by T-1. The map shows the SIP under the assumption of 270 km ionospheric height. T-1 was launched from Musudanri (black star), but its trajectory is not well known. Vertical gray line shows the time of the launch (03:07UT, Aug.31, 1998).